SAND2014-2304C

Photoresponsive Polymer Design for Solar Concentrator Self-Steering Heliostats

Jessica Barker[1], Amod Basnet[2], Moinak Bhaduri[3], Caroline Burch[4],
Amenda Chow[5], Xue Li[6], William S. Oates[7], Jordan E. Massad[8], and Ralph Smith[9]
Send correspondence to woates@fsu.edu

ABSTRACT

Concentrating solar energy and transforming it into electricity is clean, economical and renewable. One design of solar power plants consists of an array of heliostats which redirects sunlight to a fixed receiver tower and the generated heat is converted into electricity. Currently, the angles of elevation of heliostats are controlled by motors and drives that are costly and require diverting power that can otherwise be used for producing electricity. We consider replacing the motor and drive system of the heliostat with a photosensitive polymer design that can tilt the mirror using the ability of the polymer to deform when subjected to light. The light causes the underlying molecular structure to change and subsequently, the polymer deforms. The deformation of the polymer is quantified in terms of photostrictive constitutive relations. A mathematical model is derived governing the behaviour of the angle of elevation as the photostrain varies. Photostrain depends on the composition of the polymer, intensity and temperature of light and angle of light polarization. Preliminary findings show a photomechanical rod structural design can provide 60° elevation for temperatures of about 40°C. A photomechanical beam structural design can generate more tilt at lower temperatures. The mathematical analysis illustrates that photostrains on the order of 1% to 10% are desired for both rod and beam designs to produce sufficient tilt under most heliostat field conditions.

1. INTRODUCTION

Harnessing energy from the sun has become increasingly desirable as the amount of nonrenewable resources continue to decline and prices for them rise. A common solar-thermal power plant consists of an array of heliostats, central receiver and energy conversion unit as depicted in Figure 1. Physically, heliostats are mirrors attached to a base which tilts the mirror so that the sunlight is redirected to the receiver. The solar energy in the receiver is then transferred to the energy conversion unit which produces electricity.[1] The movement of the heliostats is controlled by motors and drives. This requires power that detracts from a site's energy production and they are a significant expense.

Recently, a new material composed of photoresponsive polymers has been developed which moves and twists as a result of exposure to ultra violet (UV) and visible light. We are interested in quantifying the stretching nature of these polymers as a way to configure the mirrors in heliostats. This replaces the existing complex and costly heliostat systems with a simpler system that tracks the sun. Successful implementation of photoresponsive polymers significantly reduces the cost and complexity of collecting solar energy. This project aims to design a photomechanical structure given the optical properties of sunlight encountered in a heliostat field.

We will focus mainly on the photosensitive material, azobenzene–functionalized liquid crystal polymer networks (azo-LCNs).[2] The molecular structure of azo-LCNs is illustrated in Figure 2. Light causes the molecular structure to kink and this is known as the *cis*–state (Figure 2(b)). The lowest energy molecular structure of azo-LCNs is called the *trans*–state (Figure 2(a)). The angle at the kink is approximately 45° which leads to

[1] Mathematical Sciences Department, University of Massachusetts Lowell
[2] Mathematics and Statistics Department, University of North Carolina Charlotte
[3] Mathematics Sciences Department, University of Nevada Las Vegas
[4] Mathematics Sciences Department, Clemson University
[5] Department of Applied Mathematics, University of Waterloo
[6] Mathematics Sciences Department, University of Texas at Dallas
[7] Florida State University
[8] Sandia National Laboratories
[9] North Carolina State University

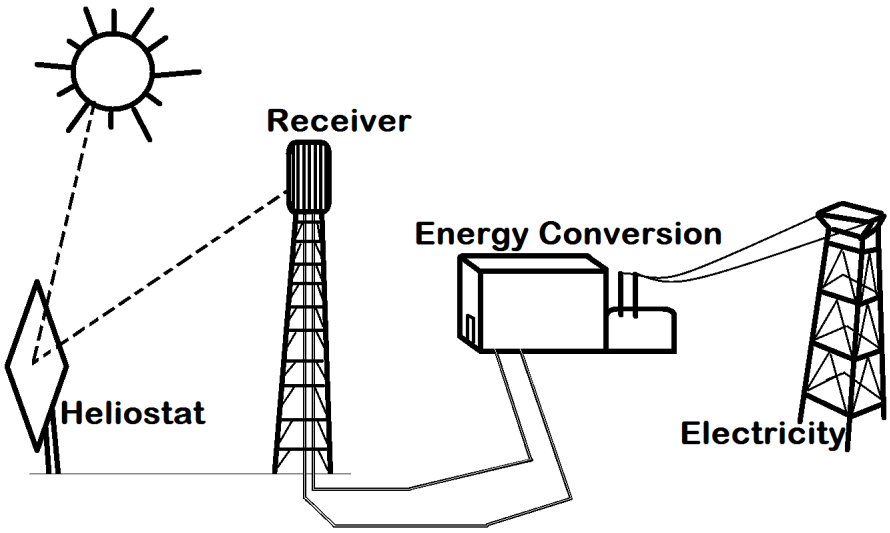

Figure 1: A common heliostat field and central receiver system that collects and transforms solar energy into electricity. This picture is modified from Figure 4.1 in Stine *et al.*[1]

a horizontal length change from 10 Angstroms in *trans*–state to 5 Angstroms in *cis*–state. The amount of *cis* concentration is due to the intensity of light directed at the material while the direction of *trans* reorientation comes from the polarization of the light. This *cis*–state causes the entire object to deform and if the material is clamped on both ends, then the material may elongate or shrink as a function of its microstructure state. This behaviour is ideal for controlling the angle of elevation of the heliostat.

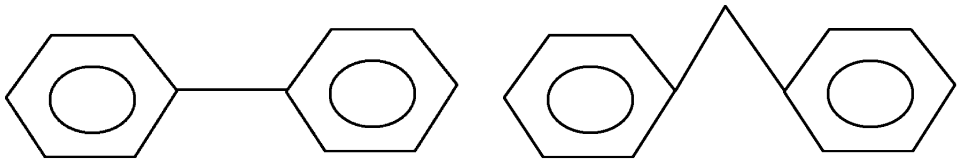

(a) *trans*–state (b) *cis*–state

Figure 2: Molecular structure of azo-LCNs. The kink angle is approximately 45° leading to a horizontal length change from 10 Angstroms in (a) to 5 Angstroms in (b).

Azo-LCNs molecules connect to form either side–chain polymers (pendants) or main–chain polymers (crosslinkers). This is displayed in Figure 3. Different ratios of pendants and crosslinkers in an azo-LCNs behave differently in response to light. This report considers 90%, 70%, 50% and 0% pendent. The more pendants in azo-LCNS, the more bending, while the more crosslinkers, the stiffer the material becomes.[3]

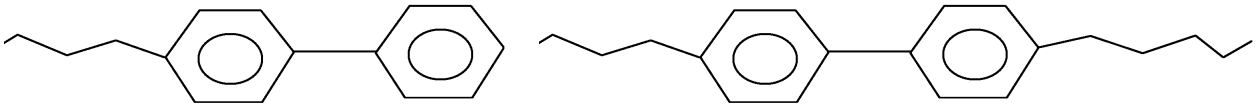

(a) Side–Chain Polymer (pendants) (b) Main–Chain Polymer (crosslinkers)

Figure 3: Conventional polymer structures of azo-LCNs.

Let ε_{xx}^{ps} and ε_{yy}^{ps} denote the surface strain induced by the photomechanical effect in the x-and y-directions, respectively, and ε_{xy}^{ps} is the shear strain. An average photostrain through the thickness of a thin sample in the y-direction is denoted as $\bar{\varepsilon}_{yy}^{ps}$ and similarly for the other two strain components.

Another behavior affected by the transformation from *cis* to *trans* state is stress, which is denoted as σ. For uni-axial loading, it is specified as

$$\sigma = Y(\varepsilon - \varepsilon^{ps})$$

where ε is the total strain, ε^{ps} is the photostrain, and Y is the Young's modulus. Typically, the stress depends on the intensity of light and Y depends on the composition and temperature of the azo-LCNs.

Sections 2 describes the behaviour of the photomechanical response. This depends on σ, Y and ε^{ps} for which mathematical equations are determined through statistical, numerical and physics based analysis. In Section 3, the angles of elevation which track the motion of the sun are determined. Section 4 and 5 provides a rod and beam design for the heliostat structure, respectively, as well as a corresponding mathematical model describing the angle of elevation in terms of the design parameters. Concluding discussions and future directions are given in the final section.

2. PHOTOMECHANICAL RESPONSE

The angle of elevation of the heliostat is determined by the polarization angle, intensity of the light, and strain of the photosensitive material. The average and surface photostrain is used for the design of a photosensitive polymer structure for the heliostat. Under fixed displacement boundary conditions, the total strain is zero $\varepsilon = 0$ and the average photostrain can be determined from blocked stress measurements and the Young's modulus as

$$\bar{\varepsilon}^{ps} = -\frac{\sigma(I)}{Y(T,c)} \tag{1}$$

where we assume the modulus depends on the intensity of light I and concentration of azobenzene c. Equations for these relationships can be determined statistically based on experimental data.

The average strain of the polymer in the x, y, and xy (shear) direction is governed by

$$\begin{aligned} \bar{\varepsilon}_{xx}^{ps} &= -\bar{\varepsilon}^{ps}\cos(2\theta) \\ \bar{\varepsilon}_{yy}^{ps} &= \bar{\varepsilon}^{ps}\cos(2\theta) \\ \bar{\varepsilon}_{xy}^{ps} &= \bar{\varepsilon}^{ps}\sin(2\theta), \end{aligned} \tag{2}$$

respectively, where θ is the light polarization angle that ranges from 0° to 90°.[2] The polarization dependence is antisymmetric with respect to 45°. This shows that photostrain can be reversed by changing polarization. Using (1) and (2), $\bar{\varepsilon}_{yy}^{ps}$ can be written as

$$\bar{\varepsilon}_{yy}^{ps} = -\frac{1}{Y(c,T)}\sigma(I)\cos(2\theta). \tag{3}$$

The y–direction is observed because the data we have is based on this direction.

Using the parameters in Table 1, we obtain the plot in Figure 4 which shows the relationship between the positive average strain, stress, and intensity from 0° to 45°. This plot indicates that the average photostrain in the y–direction increases as intensity increases and the polarization angle decreases.

Table 1: Strain parameters.

Parameter	Value	Unit
Intensity, I	(14.07, 53.19)	mW/cm^2
Young's Modulus, Y	0.92	GPa
Film Thickness, l	15	μm
Total length, h	≥ 30	μm
Polarization Angle, θ	(0, 45)	degree, $^\circ$

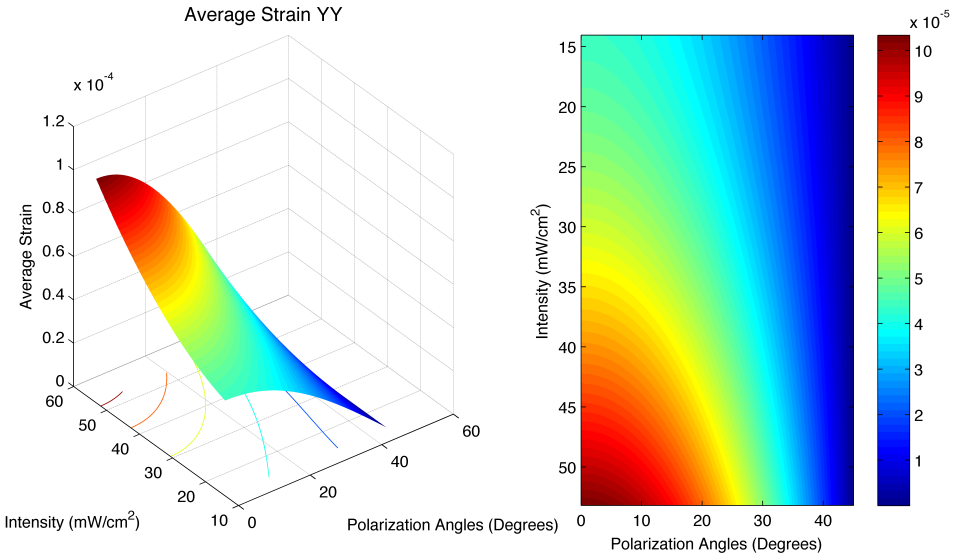

Figure 4: The relationship between average strain, stress and intensity.

3. HELIOSTAT RANGE OF MOTION

The range of motion of a heliostat dictates how much the material must deform. The range of motion is restricted to the elevation angle (angle through which the heliostat tilts to reflect the sun to the central tower) and the azimuth angle (the angle through which the heliostat twists to track the sun). Both elevation angle and azimuth angle are functions that depend on the time of day in solar time t_s, the day of the year N, the target angle λ, the facing angle ϕ, and the latitude Φ. Target angle and facing angle relate the location of the heliostat with respect to the tower as seen in Figure 5 and are measured in degrees. Similarly, latitude is measured in degrees. Solar time is measured in hours with 12 corresponding to solar noon.

To orient the elevation angle, α_E, where at a tilt of 0° the heliostat faces upward parallel to the ground, take

$$\alpha_{AE} = 90 - \alpha_E.$$

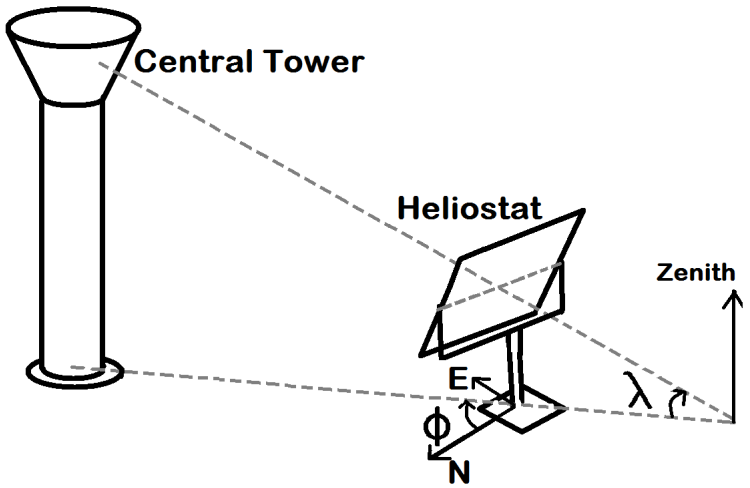

Figure 5: Coordinate system for the heliostat location in relation to the central tower where ϕ is the facing angle and λ is the target angle.

Thus, α_{AE} is the angle compared to the possible bending of the material. The elevation angle is found with the equation

$$\alpha_E = \arcsin\left(\frac{\sin\alpha + \sin\lambda}{2\cos\theta_i}\right),$$

where the sun altitude angle, α, is determined by

$$\alpha = \arcsin\left(\sin\delta\sin\Phi + \cos\delta\cos\omega\cos\Phi\right)$$

and the incident angle, θ_i, is found using the relation

$$\theta_i = \frac{1}{2}\arccos\left(\sin\alpha\sin\lambda + \cos\alpha\sin A\cos\lambda\sin\Phi + \cos\alpha\cos A\cos\lambda\cos\phi\right).$$

The declination angle δ, the hour angle ω, and the sun azimuth angle A are defined as

$$\begin{aligned}
\delta &= \arcsin\left(0.39795\cos\left(0.98563(N-173)\right)\right)\\
\omega &= 15(t_s - 12)\\
A &= \arccos\left(\frac{\sin\delta\cos\Phi - \cos\delta\cos\omega\sin\Phi}{\cos\alpha}\right).
\end{aligned}$$

These angles formulas are found in Chong and Tan.[4] All angles are measured in degrees.

The target angle is restricted to between 20° and 60°. This is an ideal arrangement for a heliostat array,[4] and solar time is restricted to between 6 and 19 hours. Latitude is set at 34.963359° and the location is the National Solar Thermal Test Facility (NSTTF) in Albuquerque, New Mexico.[5]

Figure 6 displays the range of motion for a heliostat directly north of the tower with $\lambda = 30°$. Note that the graph also includes times before and after sunset. Thus the graph shows an elevation angle of 100°; however, in practice, the maximum elevation angle needed will be less.

By taking calculations in increments of hours for t_s, days for N, 10° for λ and 45° for ϕ, the maximum angle is found to be $\alpha_{AE} = 80.85°$. This occurs for a heliostat located to the northeast and as close to the tower as allowed at sunset around the winter solstice. The minimum angle $\alpha_{AE} = 0.0584°$ occurs for a heliostat located to the southwest as far from the tower as allowed near solar noon around the winter solstice. Hence the heliostat design using the new polymer material must allow the heliostat to rotate through a range of 0° to 81° under extreme conditions. However, in many situations, solar tracking occurs only from late morning to late afternoon and heliostats are positioned mostly on one side of the receiver. Such is the case for the NSTTF, which consists of heliostats with ϕ between 90° and 180°. The results are presented in Figure 7 under these more limited conditions. Figure 7 shows approximately 60° elevation angle is needed.

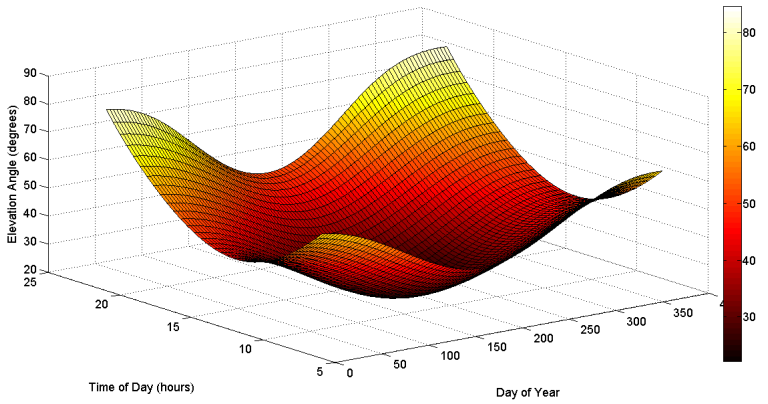

Figure 6: Range of motion for a south facing heliostat.

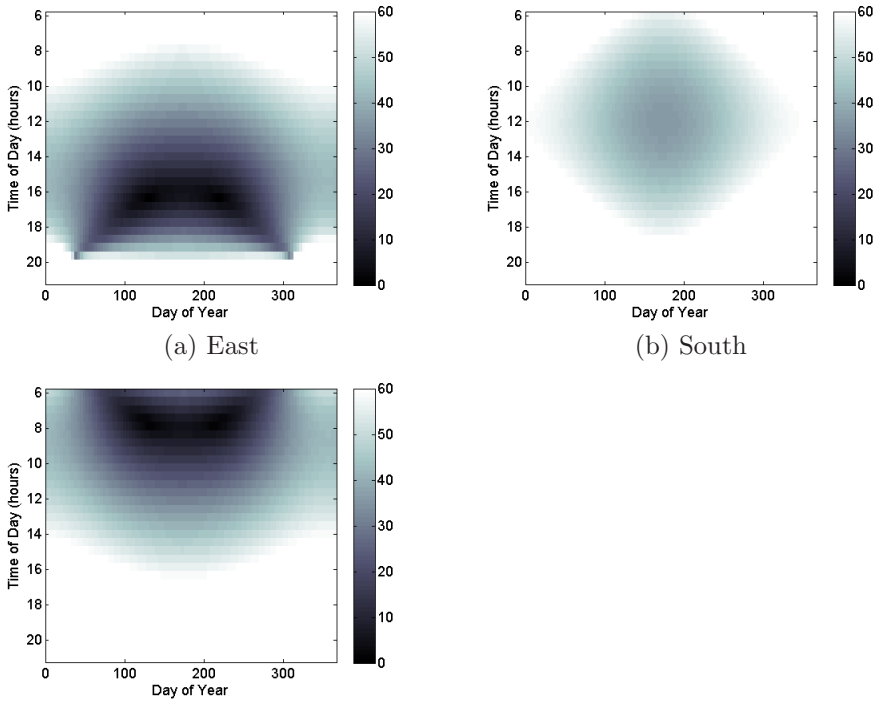

(a) East

(b) South

(c) West

Figure 7: Range of motion for a east facing, south facing, and west facing heliostat limited to 60° and below.

4. ROD HELIOSTAT DESIGN

Suppose the mirror of the heliostat is initially parallel to the ground, which is referenced as 0°. We place the mirror on a pivot and then place a rod consisting purely of the azo-LCNs a distance of r from the base of the pivot. On the other side of the pivot is a counterweight which keeps the polymer taut. The counterweight is designed to provide constant tension on the rod, since the rod has no stiffness in compression. Let L be the length of the azo-LCNs rod due to stretching and L_0 the initial length. The design parameters are L, L_0 and r, and they are measured in meters. An illustration of the heliostat structure is displayed in Figure 8.

The mechanism for the heliostat structure in Figure 8 is as follows. Sunlight activates the material that is in tension, which results in stress relaxation. In turn, the relaxation allows the counterweight to stretch the polymer from its pretensioned state and elevates the mirror. Let α_{AE} be the angle of elevation from the initial horizontal position. The angle α_{AE} is limited to 90° since at this angle, the mirror on the heliostat would be vertical and unable to reflect sunlight. It is determined in Section 3 that a physically realizable maximum angle of elevation is 81° if the heliostat is located at NSTTF in Albuquerque, New Mexico. We are interested in the behaviour of α_{AE} as the design parameters are varied.

The displacement, $u(y)$, of a rod from its original length is governed by the relation

$$\frac{\partial u}{\partial y} + \frac{1}{2}\left(\frac{\partial u}{\partial y}\right)^2 = \bar{\varepsilon}^{ps}_{yy} \tag{4}$$

where y is the position along the rod from the bottom $y = 0$ to the top $y = L_0$, and u is the positive displacement of that position from its initial state. For details on the derivation of (4), see Malvern [6, Chapter 4]. Recall that $\bar{\varepsilon}^{ps}_{yy}$ is based on equation (3) and depends on the polarization angle, light intensity, duration of light intensity and the composition of the azo-LCNs.

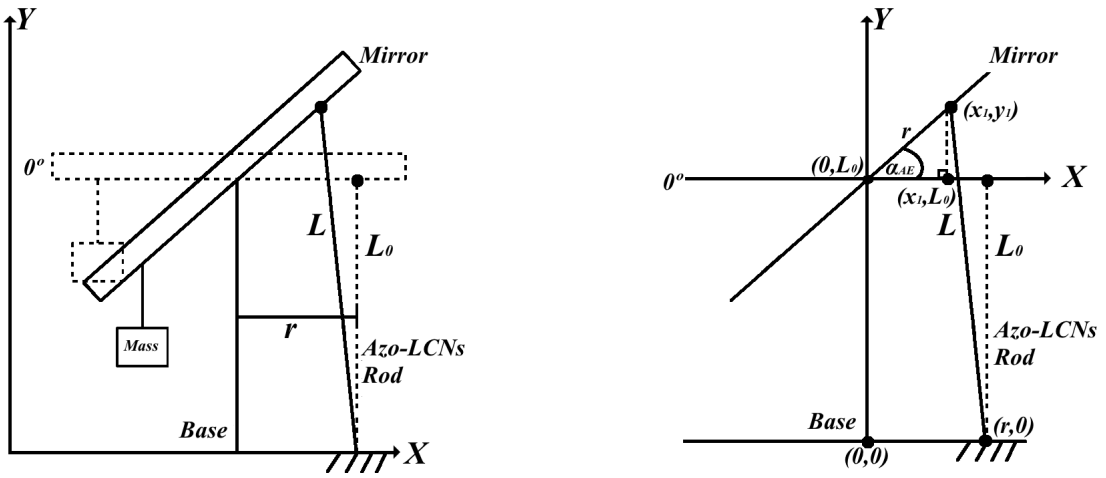

Figure 8: (a) A theoretical design for the heliostat using an azo-LCNs rod based support structure. The dashed lines represent the initial state of the heliostat. The solid lines represent the heliostat as the counterweight stretches the rod, which causes the mirror to tilt. The distance of the azo-LCN rod from the base is denoted r and the initial length of the polymer rod is L_0. The rod stretches to a length L. (b) The region around α_{AE} from Figure 8a placed on a cartesian plane.

Applying the quadratic formula to (4) gives

$$\frac{\partial u}{\partial y} = -1 \pm \sqrt{1 + 2\bar{\varepsilon}_{yy}^{ps}}$$

and integrating leads to

$$u(y) = \left(-1 \pm \sqrt{1 + 2\bar{\varepsilon}_{yy}^{ps}}\right) y + k$$

where k is the constant of integration. The displacement is $u(0) = 0$ since the bottom of the rod is fixed and hence $k = 0$. For physical reasons, $u(y)$ should be positive. It follows that the displacement of the rod is

$$u(y) = \left(-1 + \sqrt{1 + 2\bar{\varepsilon}_{yy}^{ps}}\right) y$$

for all y. Since L and L_0 are varying in the heliostat rod model and the initial length is L_0, then

$$L(L_0) = \left(-1 + \sqrt{1 + 2\bar{\varepsilon}_{yy}^{ps}}\right) L_0 + L_0. \tag{5}$$

Values of $\bar{\varepsilon}_{yy}^{ps}$ are based on experiments on the azo-LCNs clamped at both ends in a pretensioned state.[2] This is analogous to the counterweight applied to the azo-LCNs rod and hence initially the azo-LCNs in the heliostat structure is pretensioned. In future designs, the counterweight can be used as a design parameter to adjust the pretensioned state. Mathematically, the initial displacement would depend on the weight of the counterweight.

Elementary geometry provides a relationship between α_{AE} and the design parameters. We reference the origin to be the point where the base is stationed to the ground. Let $(r, 0)$ be the point in which the bottom of the rod is stationed to the ground and (x_1, y_1) is the point of intersection between the mirror and the stretched rod. See Figure 8b for a visual interpretation. The distance from $(r, 0)$ to (x_1, y_1) is

$$(x_1 - r)^2 + (y_1)^2 = L^2$$

and

$$\sin(\alpha_{AE}) = \frac{y_1 - L_0}{r} \qquad \text{and} \qquad \cos(\alpha_{AE}) = \frac{x_1}{r}.$$

It follows that

$$r^2\left(\cos(\alpha_{AE})-1\right)^2+\left(r\sin(\alpha_{AE})+L_0\right)^2=L^2$$

and substituting in (5) leads to

$$r^2\left(\cos(\alpha_{AE})-1\right)^2+\left(r\sin(\alpha_{AE})+L_0\right)^2=\left(1+2\bar{\varepsilon}_{yy}^{ps}\right)L_0^2. \tag{6}$$

Denote the ratio $\rho=r/L_0$. This is always defined as L_0 must be nonzero. Expanding the squares in (6) and writing in terms of ρ gives

$$\rho^2\left(1-\cos(\alpha_{AE})\right)+\rho\sin(\alpha_{AE})=\bar{\varepsilon}_{yy}^{ps} \tag{7}$$

Rewriting (7) in terms of only $\sin(\alpha_{AE})$, the equation becomes

$$\rho^2\left(1-\left(1-\sin^2(\alpha_{AE})\right)^{1/2}\right)+\rho\sin(\alpha_{AE})=\bar{\varepsilon}_{yy}^{ps}$$

and using the quadratic formula to solve for $\sin(\alpha_{AE})$ leads to

$$\sin(\alpha_{AE})=\frac{-\left(\rho^2-\bar{\varepsilon}_{yy}^{ps}\right)\pm\rho\sqrt{\rho^2\left(1+2\bar{\varepsilon}_{yy}^{ps}\right)-\left(\bar{\varepsilon}_{yy}^{ps}\right)^2}}{\rho\left(\rho^2+1\right)}.$$

It follows that

$$\alpha_{AE}=\arcsin\left(\frac{-\left(\rho^2-\bar{\varepsilon}_{yy}^{ps}\right)+\rho\sqrt{\rho^2\left(1+2\bar{\varepsilon}_{yy}^{ps}\right)-\left(\bar{\varepsilon}_{yy}^{ps}\right)^2}}{\rho\left(\rho^2+1\right)}\right). \tag{8}$$

The "positive" solution is chosen since graphically it coincides with (7) and numerical studies show the "negative" solution gives negative angles of elevation.

From equation (8), it is clear that restrictions on ρ and $\bar{\varepsilon}_{yy}^{ps}$ are needed to ensure a physically valid angle of elevation. The condition

$$\rho\geq\frac{\bar{\varepsilon}_{yy}^{ps}}{\sqrt{1+2\bar{\varepsilon}_{yy}^{ps}}} \tag{9}$$

ensures a real solution of (8). Within a valid range of design parameters, numerical studies show that there is no upper bound on ρ to ensure physical solutions to (8). Equation (8) provides the angle of elevation restricted from 0° to 90° a function of the photostrain $\bar{\varepsilon}_{yy}^{ps}$ which is determined by (3) and the rod design, ρ, subject to (9).

Equation (8) is plotted in Figure 9. Note that if MATLAB provided not a number as a result for the angle of elevation, that effectively means $\alpha_{AE}=0$. It is clear from the figure that as both $\bar{\varepsilon}_{yy}^{ps}$ and ρ increases, the angle of elevation increases. Experiments show that the maximum photosensitive strain for azo-LCNs is approximately 0.01.[2] It is clear from Figure 9 that only a small angle of elevation is achieved at this level of $\bar{\varepsilon}_{yy}^{ps}$, thus we also consider a beam design to explore large bending actuation capabilities.

5. BEAM HELIOSTAT DESIGN

The azo-LCNs beam is fixed at one end to a support base and on the other end the mirror of the heliostat is attached. The length of the beam is $L=L_0$ and changes negligibly unlike in the rod model where L and L_0 are differing values. Initially the mirror is parallel to the support. This means the angle of elevation is 0°. As the sunlight is directed onto the beam, it bends upwards; that is, the angle of elevation is increasing. This is displayed in Figure 10 in a rotated orientation.

Figure 11 represents a beam structure with two layers of film. The active layer and the inactive layer are represented by A and I, respectively. The active layer responds to the light causing it to either contract or expand depending on the composition of the polymer. Light has no effect on the inactive layer. We assume that upon incident of light, the active layer contracts causing the beam to bend upward as shown in Figure 10.

Let h and b be the thickness and the width of the composite structure, respectively. We assume both the active and the inactive layer have the same modulus, $Y_A=Y_I$, and same thickness, $h/2$. Denote z_n as the neutral

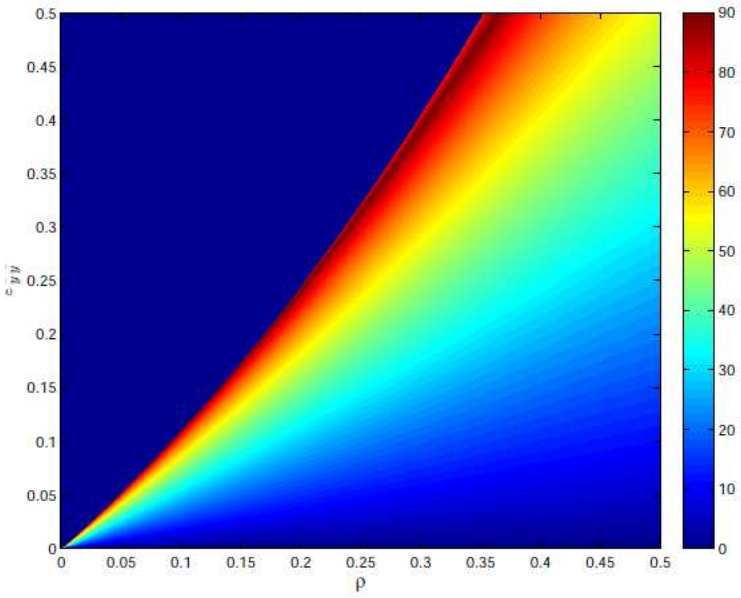

Figure 9: A plot of equation (8) which governs the behavior of α_{AE} as ρ and $\bar{\varepsilon}^{ps}_{yy}$ varies. The vertical bar on the right represents α_{AE}, which is measured in degrees.

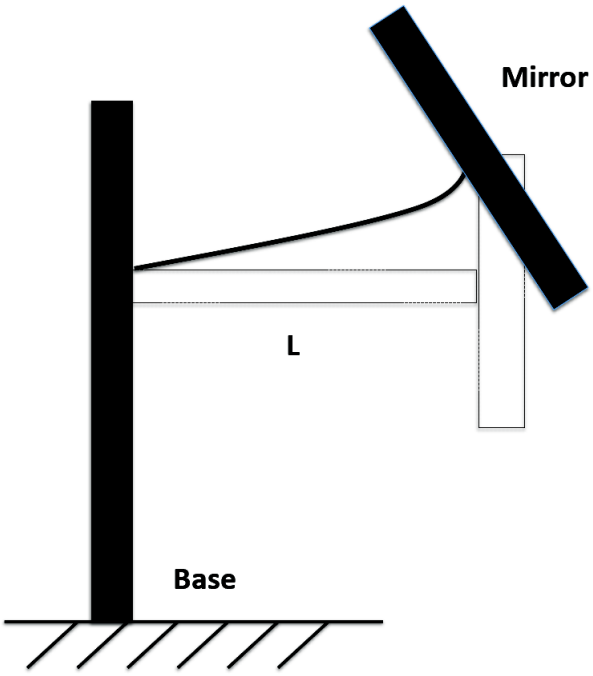

Figure 10: Heliostat structure using a beam design where L is the length of the beam.

line where $\varepsilon(z_n) = 0$. Because the beam is homogenous, then $z_n = 0$. We assume that light is uniformly incident on the film and is uniformly distributed over the surface of the film for a particular thickness z. Since σ_{yy} is in the negative y-direction, the active layer contracts, as a result, the beam bends upward.

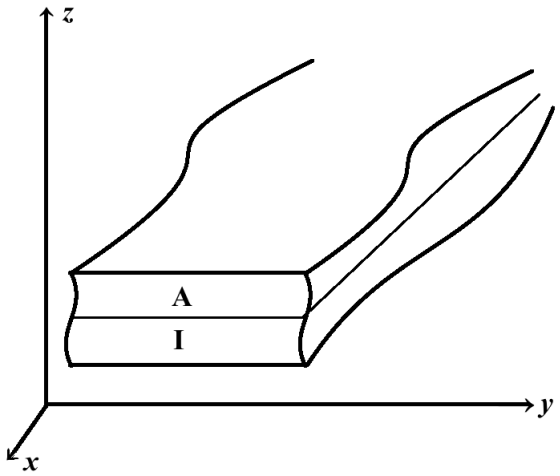

Figure 11: A bi-layer beam with active layer A and inactive layer I.

The moment induced by light is given by

$$\begin{aligned} M_{\text{light}} &= -b\int_0^{h/2}(Y\varepsilon_{yy}^{pl})z\,dz \\ &= -bY\frac{h^2}{8}\varepsilon_{yy}^{pl} \end{aligned} \tag{10}$$

where the relation between the thickness averaged strain, ε_{yy}^{pl}, and ε_{yy}^{ps} is given in Dunn *et al.* [7, equation (6)] as

$$\varepsilon_{yy}^{pl} = \frac{(\exp(\frac{h}{l})-1)^2\varepsilon_{yy}^{ps}}{2\left(l(\exp(\frac{h}{l})-1)-h\right)\exp(\frac{h}{l})}.$$

The characteristic length associated with light attenuation, l, typically ranges from 10 to 20μm. For nominal values for azobenzene, l is 15μm. Given our assumption that light is uniform, a pure moment is generated which

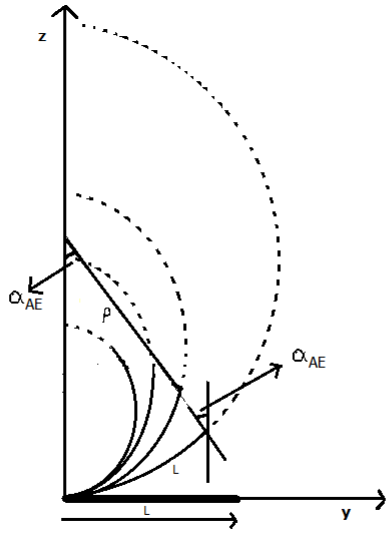

Figure 12: Bending behavior of the beam subject to varying photo-stress.

gives rise to a smooth curvature. We assume bending follows a circular path with varying radius of curvature, ρ, which depends on ε_{yy}^{pl} and the design parameters. The geometry of the bending is shown in Figure 12.

The moment of the active layer due to strain ε_{yy}^{pl} is governed by

$$M_{\text{light}} = \frac{YI}{\rho} \tag{11}$$

$$\rho = \frac{YI}{M_{\text{light}}} \tag{12}$$

$$\kappa = \frac{M_{\text{light}}}{YI}. \tag{13}$$

Substituting equation (10) into equation (12), the relation $\alpha = L/\rho$ and the expression for ε_{yy}^{pl}, it follows that

$$\alpha_{AE} = \frac{3}{2}\frac{l}{h}\varepsilon_{yy}^{pl} = \frac{3}{4}\frac{l}{h}\frac{(\exp(\frac{h}{l})-1)^2\varepsilon_{yy}^{ps}}{\big(d(\exp(\frac{h}{l})-1)-h\big)\exp(\frac{h}{l})}.$$

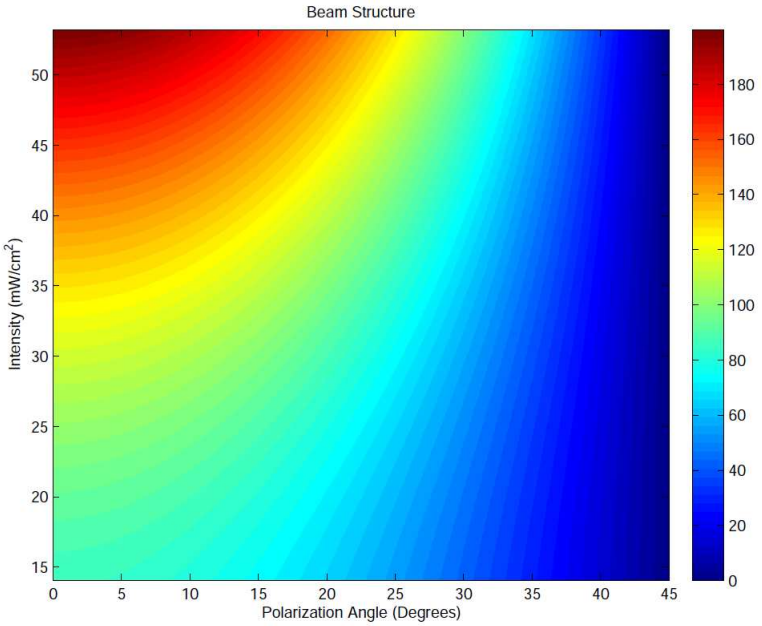

Figure 13: Variation of α_{AE} as a function of intensity of light and polarization angle for $L = 10$ cm and $h = 30\mu$m.

We assume that the active layer and the inactive layer have thickness h_1 and h_2, respectively. The combined thickness of the film is h. The moment of the active layer is given by

$$\begin{aligned} M_{\text{light}} &= -b\int_{h/2-h_1}^{h/2}(Y\varepsilon_{yy}^{pl})z\,dz \\ &= -bY\frac{h_1(h-h_1)}{2}\varepsilon_{yy}^{pl}. \end{aligned}$$

Using the relation in (12) and ε_{yy}^{ps}, the tilt of the mirror is given by

$$\alpha_{AE} = \frac{6Lh_1(h-h_1)}{h^3}\frac{(\exp(\frac{h}{l})-1)^2 l}{2(l(\exp(\frac{h}{l})-1)-h)\exp(\frac{h}{l})}\varepsilon_{yy}^{ps}. \tag{14}$$

The thickness of the active layer h_1 depends on the material parameter l and thickness h. The relation between h_1, l and h is based on Dunn *et al.* [7, equation (6)],

$$h_1 = 2\frac{(l\exp(\frac{h}{l}) - 1) - h}{(\exp(\frac{h}{l}) - 1)}.$$

Taking the limit for sufficiently large h implies h_1 approaches $2l$. This establishes an upper limit for h_1. Substituting the expression for h_1 into (14) gives

$$\alpha_{AE} \quad = \quad \frac{6Ll}{h^3\exp(\frac{h}{l})}\left((\exp(\frac{h}{l}) - 1)(h - 2l) + 2h)\right)\varepsilon_{yy}^{ps}. \tag{15}$$

From (15), taking the limit for sufficiently large h, we obtain

$$\lim_{h\to\infty}\alpha_{AE} = \lim_{h\to\infty}\frac{\exp(\frac{h}{l})}{h^2\exp(\frac{h}{l})} = \lim_{h\to\infty}\frac{1}{h} = 0.$$

Qualitatively, as the thickness of the beam becomes very large, the tilt of the mirror gets smaller. Equation (15) shows some linear relations with respect to L and ε_{yy}^{ps}.

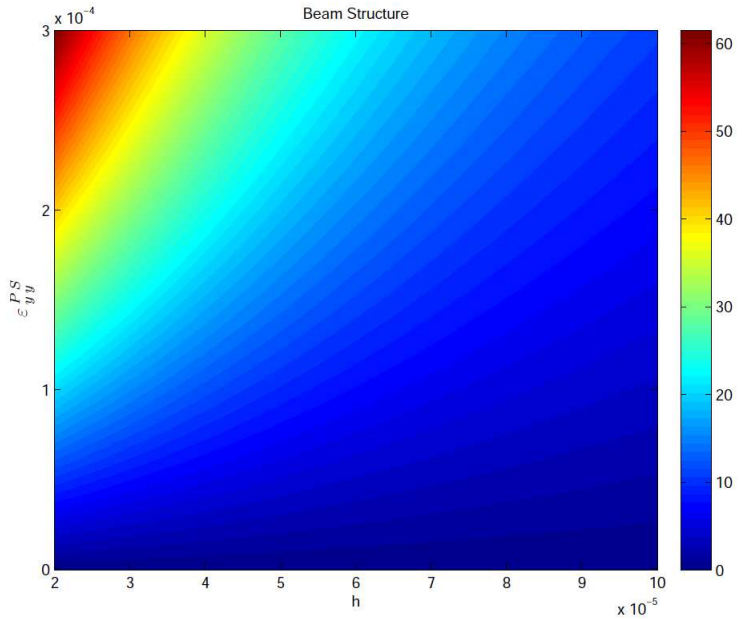

Figure 14: The thin beam structure for the variation of α_{AE} as a function of ε_{yy}^{ps} and thickness of the beam for $L = 0.1$ cm.

The change in α with respect to polarization angle and intensity of light is shown in Figure 13. Observe that the value of α_{AE} is significant if the polarization angle is small at any given intensity. We can conclude if light is polarized in the same direction as the molecules in the active layer, we expect to observe the maximum tilting of the mirror.

The variation of α_{AE} as a function of ε_{yy}^{ps} and thickness is shown in Figures 14 and 15. It is observed that as the thickness of the beam increases, α_{AE} decreases which is consistent with the theory. Therefore, we can expect to increase α_{AE} by using a beam with a small thickness. If the beam is thin enough, in the order of μm, then little strain is required to cause it to bend significantly as shown in Figure 14. However, if the beam is to hold a mirror, the thin beam structure would not be feasible. The results in Figure 15 depicts a beam with increased thickness (in the order of millimeters). Notice that at least 5% to 10% strain leads to an α_{AE} between 30° to 60°.

We note that the mirror is assumed to be massless. The choice for L requires careful consideration from an engineering feasibility point of view. To establish a realistic design that caters to a complete structural design, we have to consider the mass of the mirror. The moment of the mirror was not considered for the model described above. In addition to the moment as a result of photo-stress, the moment due to the mirror acts in the opposite direction. If this is factored in, we will be able to obtain a constraint for the length as well as thickness of the mirror.

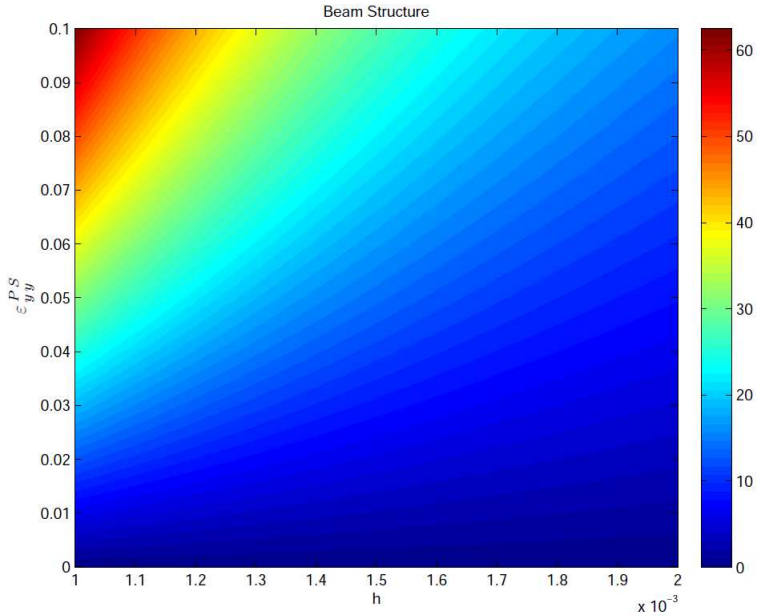

Figure 15: Thick beam structure for the variation of α_{AE} as a function of ε_{yy}^{ps} and thickness of the beam for $L = 12.5$ cm.

6. DISCUSSION

A number of factors influence the angle of elevation such as the intensity and polarization of light, Young's modulus, composition of the azo-LCNs, length of the rod or beam structure, and available strain. At least 60° tilt is needed to orient a heliostat. This requires at least 5% photostrain for the rod. In general, a large strain is required to provide sufficient angles of elevation, but existing material performance may be insufficient in glassy polymer compositions. To maximize the photostrain in azo-LCNs, additional work is required to determine material compositions (e.g., glassy versus elastomer compositions) that are ideal for heliostat applications. For example, it is shown that azobenzene elastomeric materials have a maximum value of $\bar{\varepsilon}_{yy}^{ps} \simeq 20\%$.[8]

Currently the design for the heliostat rod is theoretical. Improvements to the design is needed such as including the azimuth angle and the weight of the mirror. Experimental testing is needed to validate the optimal design for heliostat structures. A beam structure may be a more efficient model than a rod structure. Furthermore, in future research the equations discussed in this paper can be used to control the angle of elevation.

REFERENCES

[1] Stine, W. B., Wilkins, F., Scheve, M., Gronich, S., Leonard, J., Heckes, A., Skinrod, Al Radosevich, L., Vant-Hull, L., Holl, R., Tracey, T., and LaPorta, C., [*Power from the Sun*], Solar Energy Research Institute (1987).

[2] Cheng, L., Torres, Y., Lee, K. M., McClung, A., Baur, J., White, T., and Oates, W., "Photomechanical bending mechanics of polydomain azobenzene liquid crystal polymer network films," *J. Appl. Phys. (USA)* **112**(1), 013513 (16 pp.) (2012).

[3] Worden, M., Wang, H., Paravastu, A., and Oates, W., "Macro and molecular scale experimental characterization of the photomechanics of azobenzene polymer networks," *Smart Material Structure* (Submitted).
[4] Chong, K. and Tan, M., "Range of motion study for two different sun-tracking methods in the application of heliostat field," *Solar Energy* **85**(9), 1837–1850 (2011).
[5] Map, "Google maps," (July 2013).
[6] Malvern, L. E., [*Intoduction to the Mechanics of a Continuous Medium*], Prentice-Hall (1969).
[7] Dunn, M., "Photomechanics of mono- and polydomain liquid crystal elastomer films," *J. Appl. Phys. (USA)* **102**(1), 13506 – 1 (2007).
[8] Finkelmann, H., Nishikawa, E., Pereira, G., and Warner, M., "A new opto-mechanical effect in solids," *Phys. Rev. Lett. (USA)* **87**(1), 015501 – 1 (2001).